

Blackbody Radiation from Hot Two-Dimensional Electrons in AlGaAs/GaAs Heterojunctions

AlGaAs/GaAs ヘテロ構造中の 2 次元ホットエレクトロンからの黒体放射

Kazuhiko HIRAKAWA*

平川 一彦

We have studied the broad-band far-infrared (FIR) radiation from hot two-dimensional (2D) electrons in selectively doped AlGaAs/GaAs heterojunctions. The combination of a composite Si-bolometer and a magnetic-field tuned InSb cyclotron resonance filter allows us a spectroscopic as well as an intensity analysis of the FIR emission from hot 2D electrons. It is found that the radiation spectra are well explained by the theory of blackbody radiation and the emissivity assuming a classical Drude conductivity. The behavior of the determined effective blackbody temperatures of hot 2D electrons is quantitatively explained by a theory of acoustic and optical phonon emissions.

1. INTRODUCTION

The two-dimensional (2D) electrons in selectively-doped AlGaAs/GaAs heterojunctions exhibit very high mobility,^{1,2)} because of the spatial separation of electrons from their parent donors in the AlGaAs. Advantages of using such a high mobility system are well recognized and applied to high-speed field-effect transistors (FETs).³⁾ The high mobility 2D electrons are, however, easily heated up by an external electric field, leading to a rapid rise in electron temperature and a reduction of electron mobility. Such a "hot electron" effect is one of the most important issues in practical device applications. The experimental approach which can characterize the electron temperature (T_e), however, has been limited so far; although the analysis of Shubnikov-de Haas (SdH) oscillations allows an accurate and sensitive determination of T_e ,^{4,5)} it is applicable only up to $T_e \sim 20$ K. The analysis of the high-energy tail of photoluminescence (PL) spectra^{6,7)} is, on the other hand, good for high T_e 's, but it becomes inapplicable below ~ 25 K due to finite non-thermal PL line width. Also, PL method has a drawback that it cannot be used for the single interface structure, which is the more widely used structure in the

FET applications.

In this work, we have studied broad-band far-infrared (FIR) radiation from hot 2D electrons in selectively doped AlGaAs/GaAs heterojunctions. An electron system at temperature T_e is expected to emit blackbody radiation of equivalent temperature. Since blackbody radiation is a direct consequence of velocity fluctuation of electrons, it gives a good measure of thermodynamic temperature of the electron system without postulating a specific type of distribution function for the electrons. This fact is quite important in high electric field transport, where electron distribution function could be strongly deformed from its equilibrium form, *i. e.* the Fermi-Dirac distribution function. The combination of a wide-band FIR detector and a magnetic-field tuned InSb cyclotron resonance (CR) filter⁸⁾ allows us a spectroscopic analysis of the FIR emission from hot 2D electrons. It is found that the radiation spectra are, indeed, well explained by the theory of blackbody radiation, which enables us to determine the effective blackbody temperature, or the 2D electron temperature T_e . The integrated intensity of the blackbody radiation, I_b , is proportional to T_e^γ , the exponent γ gradually decreasing from 4 to ~ 2 with increasing electron mobility μ . Since I_b is strongly dependent on T_e , T_e has been determined sensitively for a wide temperature range (5~100 K). We also discuss

*Center for Function Oriented Electronics, Institute of Industrial Science, University of Tokyo

the dominant energy relaxation mechanism of hot 2D electron system.

2. EXPERIMENTAL

The samples used in this study are AlGaAs/GaAs single interface heterojunctions grown by either molecular beam epitaxy or liquid phase epitaxy. Each sample was cut into $\sim 2.5 \times 3.5 \text{ mm}^2$ piece and ohmic contacts for source, drain, and voltage probes were made by alloying InSn. The low-field transport parameters (electron densities N_s and mobilities μ) at lattice temperature $T_L = 4.2 \text{ K}$ were determined by in-situ magnetotransport measurement and are listed in Table I. A composite Si-bolometer operated at 1.5 K was used as a wide-band FIR detector to measure the broad-band FIR emission from the samples. The CR absorption of a high-purity InSb slab was used as a tunable filter for spectroscopy.⁸⁾ The energy position E_{CR} and the line width $\Delta\hbar\omega$ of the InSb CR were calibrated by using a Fourier transform spectrometer. $\Delta\hbar\omega$, which limits our spectral resolution, is 3 meV (5~7 meV) when E_{CR} is below (above) the Reststrahl band (22.8–24.4 meV) of InSb. The responsivity of the measurement system, including FIR waveguides and a sapphire window, was calibrated to be $1 \times 10^5 \text{ V/W}$ by measuring the blackbody radiation from a NiCr-film heater/AuGe thermometer device.⁹⁾ Because of the presence of a sapphire window, our system is sensitive up to $\sim 370 \text{ cm}^{-1}$ ($\sim 45 \text{ meV}$). In the experiment, hot electrons were excited by applying 0.7 ms-long voltage pulses¹⁰⁾ to the ohmic contacts on two ends of the samples and the bolometer signal was detected by using a box-car averager. The duty ratio of the pulses was maintained below 1/100 to minimize lattice heating. All the experiments were performed at $T_L = 4.2 \text{ K}$.

Table I Electron densities and low field mobilities of the samples at 4.2 K.

sample	$N_s \text{ (cm}^{-2}\text{)}$	$\mu \text{ (cm}^2\text{/Vs)}$
#1	4.4×10^{11}	3.7×10^4
#2	3.3×10^{11}	1.1×10^5
#3	3.1×10^{11}	2.2×10^5

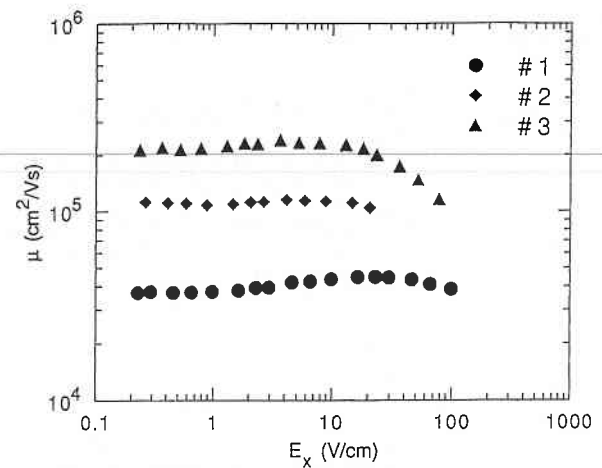


Fig. 1 The dependence of electron mobilities μ on applied electric fields E_x .

First, we characterized the electron mobilities μ as a function of applied electric field E_x by in-situ pulsed I - V measurements. As shown in Fig. 1, μ initially increases slightly with increasing E_x , suggesting that the ionized impurity scattering becomes less effective as T_e rises.¹¹⁾ However, μ eventually starts to decrease with E_x and asymptotically approaches the line limited by a saturation velocity.¹¹⁾

3. SPECTROSCOPY OF BROADBAND FIR RADIATION FROM HOT ELECTRONS

We measured the spectra of FIR emission from hot 2D electrons excited by applying voltage pulses. Between the samples and the Si-bolometer, a wedged InSb slab was inserted at the center of the superconducting solenoid and its CR energy was swept by applying a magnetic field. The samples were mounted 25 cm-above the center of the magnet (see the inset of Fig. 2); the residual magnetic field at the sample position was kept less than 600 Gauss. Fig. 2 shows typical FIR emission spectra from the hot 2D electrons. In the figure, the magnetic field applied to the InSb filter is converted to its CR energy. It is found that the FIR emission spectra from hot 2D electrons are broad and, for higher excitations, both the intensity and the width of the emission increase.

In thermal equilibrium, the spectral emission intensity per solid angle $i_b(\omega)$ of the FIR radiation from a system with temperature T is given by¹²⁾

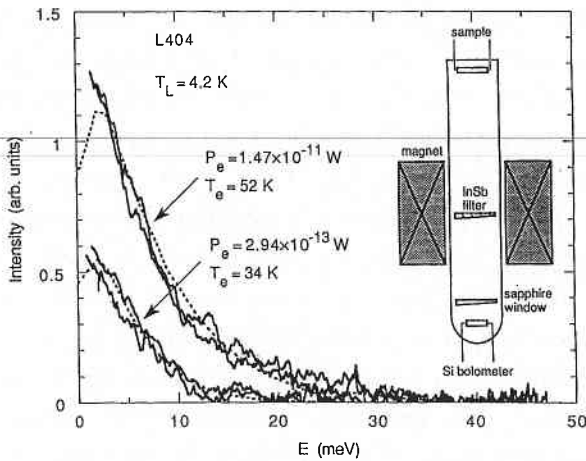


Fig. 2 Far Infrared emission spectra from hot two-dimensional electrons measured by using a magnetic-field-tuned InSb cyclotron resonance (CR) filter. The magnetic field applied to the filter has already been converted to the CR energy. Also plotted by dotted lines are the theoretical curves for blackbody radiation which are calculated by Eq. (3) and convoluted with the InSb filter transmission function. The inset shows a schematic illustration of the experimental setup for the spectroscopic measurement.

$$i_b(\omega) d\omega d\Omega = i_{bb}(\omega) A(\omega, \theta) \cos \theta d\omega d\Omega, \quad (1)$$

where $i_{bb}(\omega)$ is the spectral emission intensity of a real blackbody, Ω the solid angle, and $A(\omega, \theta)$ the incident-angle (θ)-dependent spectral absorptivity of the system; in equilibrium, the emissivity and the absorptivity are equivalent. For example, for an AlGaAs/GaAs single interface 2D electron system, $A(\omega, \theta)$ for normal incidence is expressed as¹³⁾

$$A(\omega, \theta = 0) = \frac{4 \operatorname{Re}(F)}{|+\sqrt{\kappa} + F|^2}, \quad (2)$$

where $F = \sigma(\omega) / \epsilon_0 c$ with $\sigma(\omega)$ the dynamical conductivity of the 2D electrons, ϵ_0 the dielectric permittivity of vacuum, κ the dielectric constant of GaAs, and c the speed of light. The blackbody radiation intensity per unit area, $I_b(\omega)$, can be written as¹²⁾

$$I_b(\omega) d\omega = \int \frac{\hbar \omega^3}{4\pi^3 c^2 [\exp(\hbar \omega / k_B T) - 1]} A(\omega, \theta) \cos \theta d\omega d\Omega, \quad (3)$$

with k_B the Boltzmann constant. In the following discussion, we made two assumptions; (i) we assume that Eq. (3) is valid even in non-equilibrium steady-state condition, and (ii) we assume a classical Drude conductivity for $\sigma(\omega)$, *i. e.*

$$\sigma(\omega) = \frac{e^2 N_s \tau_m}{m^*} \frac{1}{1 - i\omega\tau_m}, \quad (4)$$

with e the electronic charge and τ_m the E_x -dependent momentum-relaxation time which is determined by I - V measurement.

We calculated the blackbody radiation spectra by using Eq. (3) and convoluted them with the line shape function of the InSb CR peak. For the blackbody temperature of 2D electrons in Eq. (3), we used the values determined from the integrated intensity of the radiation, as described in the next section. The calculated spectra are plotted as dotted lines in Fig. 2, and show a good agreement with the experimental data, which confirms that the broadband radiation from the hot 2D electrons is indeed of the blackbody radiation origin. This fact enables us to deduce the thermodynamic blackbody temperature, or the electron temperature T_e , of the hot 2D electrons from the FIR emission data.

4. DETERMINATION OF THERMODYNAMIC TEMPERATURE OF ELECTRON SYSTEM

We next measured the integrated intensity of the broadband FIR emission, I_b , to determine T_e more sensitively. I_b is defined as

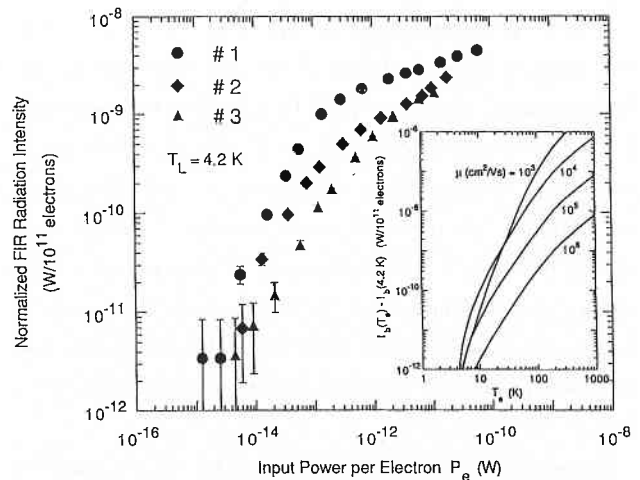


Fig. 3 The normalized FIR emission intensities are plotted as functions of input electrical power per electron P_e . The inset shows the normalized blackbody radiation intensities calculated as functions of the electron temperature for different μ_s .

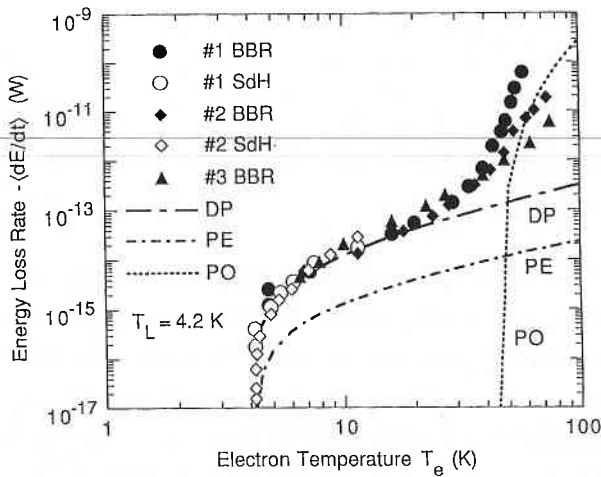


Fig. 4 The determined electron temperatures T_e versus the energy loss rates of two-dimensional electrons, which is equivalent to T_e in a steady state. Full and open symbols denote FIR (plotted as BBR) and magnetotransport (plotted as SdH) results, respectively. Calculated energy loss rates due to phonon emissions are also shown by dashed and dotted lines; DP the deformation potential interaction, PE the piezoelectric interaction, and PO the polar optical phonon interaction.

$$I_b = \int_{\omega_{\min}}^{\omega_{\max}} I_b(\omega) d\omega, \quad (5)$$

where ω_{\min} and ω_{\max} are the low and high cut-off frequencies of the FIR detection system and $\sim 5 \text{ cm}^{-1}$ and $\sim 370 \text{ cm}^{-1}$ in our case, respectively. As shown in the inset of Fig. 3, the calculated I_b is approximately proportional to T_e^γ , the exponent γ gradually decreasing from 4 to ~ 2 with increasing μ . The decrease of γ with μ is due to the high-frequency cut-off of the FIR radiation by longer τ_m . Since I_b is strongly dependent on T_e , sensitive determination of T_e is possible by comparing I_b with theoretical calculations. This method is more sensitive than that used by Hopfel *et al.*¹³⁾ and Okisu *et al.*¹⁴⁾; they measured the spectral emission intensity $I_b(\omega)\Delta\omega$ at a fixed frequency by using narrow-band crystal detectors with band widths $\Delta\omega$ ($\sim 2 \text{ cm}^{-1}$) and $I_b(\omega)$ is approximately proportional to T_e .

To measure I_b , the InSb filter was removed and the FIR radiation was directly detected by the Si-bolometer. In Fig. 3, the measured emission intensities which are normalized by N_s and the sample area S , I_{bn} ($\equiv I_b/N_s S$), are plotted as functions of input electrical power per electron P_e (\equiv

$J_x E_x / N_s$ with J_x the current density). It is noted that I_{bn} increases rapidly with increasing P_e in the low excitation region and shows a saturation behavior for higher P_e . It is also noted that I_{bn} is larger for lower mobility sample, as expected from Eqs. (2) and (4); *i. e.*, the lower mobility sample has higher emissivity in the FIR frequency range. By comparing the measured I_{bn} with theoretical values calculated by using Eqs. (2)-(5) and the calibrated detector responsivity, it is possible to determine T_e of hot 2D electrons. In Fig. 4, the determined T_e 's are plotted by filled symbols versus the energy loss rate $-dE/dt$, which is equivalent to P_e in steady states. In the figure, T_e 's determined by analyzing the amplitude of SdH oscillations measured on the identical samples in the same experimental run are also plotted by open symbols. It is noted that the FIR emission method can detect a temperature rise as small as $\sim 2 \text{ K}$ and can cover up to $\sim 100 \text{ K}$ range.¹⁵⁾ It is also noted that the FIR emission data and the magnetotransport data agree well with each other where they overlap, suggesting the accuracy of the FIR emission method.

As seen in Fig. 4, T_e rises rapidly with P_e and reaches 40 K when $P_e \sim 10^{-13} \text{ W}$. For $P_e > 10^{-13} \text{ W}$, however, T_e shows a drastic change in slope, indicating an onset of another energy relaxation mechanism. In order to understand the energy relaxation mechanisms, we calculated the energy loss rates due to acoustic and optical phonon emissions within a framework of the electron temperature model. In the calculation, we used the Fang-Howard variational wave function¹⁶⁾ and assumed that only the lowest subband is occupied. The detail of the calculation has been published elsewhere.¹⁷⁾ The calculated energy loss rates for $N_s = 5 \times 10^{11} \text{ cm}^{-2}$ are also plotted in Fig. 4. The excellent agreement between the experimental and theoretical results indicates that the dominant energy relaxation mechanism for $T_e < 40 \text{ K}$ is the acoustic phonon emission via deformation potential coupling, while optical phonon emission becomes a much more efficient electron cooling mechanism when $T_e > 40 \text{ K}$. It is also noted that the rise in T_e is almost independent of N_s when $T_e < 40 \text{ K}$, which is a characteristic of the screened acoustic phonon interaction.¹⁷⁾

5. CONCLUSIONS

In summary, we studied the broad-band FIR radiation from hot 2D electrons in selectively doped AlGaAs/GaAs heterojunctions. By using a wide-band Si-bolometer and a magnetic-field tuned InSb cyclotron resonance filter, we performed a spectroscopic analysis of the FIR emission from hot 2D electrons. It is found that the radiation spectra are well explained by the theory of blackbody radiation, and the thermodynamic temperature of the hot 2D electron system has been successfully determined from 5 K to 100 K. The behavior of the determined electron temperature is quantitatively explained by a theory of acoustic and optical phonon emissions.

ACKNOWLEDGMENTS

This work was done in collaboration with Prof. D. C. Tsui, M. Grayson, and C. Kurdak of Princeton University. Thanks are also due to Dr. R. J. Wagner of Naval Research Laboratory for high purity InSb wafers and to Prof. T. Ikoma for molecular-beam-epitaxially grown samples.

(Manuscript received, December 3, 1992)

References

- 1) H. L. Stormer, R. Dingle, A. C. Gossard, W. Wiegmann, and M. D. Sturge, *Solid State Commun.* **29**, 705 (1979).
- 2) For example, L. Pfeiffer, K. W. West, H. L. Stormer, and K. W. Baldwin, *Appl. Phys. Lett.* **55**, 1888 (1988).
- 3) T. Mimura, S. Hiyamizu, T. Fujii, and K. Nanbu, *Jpn. J. Appl. Phys.* **19**, L225 (1980).
- 4) F. F. Fang and A. B. Fowler, *J. Appl. Phys.* **41**, 1825 (1970).
- 5) H. Sakaki, K. Hirakawa, J. Yoshino, S. P. Svensson, Y. Sekiguchi, T. Hotta, and S. Nishi, *Surf. Sci.* **142**, 306 (1984).
- 6) J. Shah, A. Pinczuk, H. L. Stormer, A. C. Gossard, and W. Wiegmann, *Appl. Phys. Lett.* **42**, 55 (1983); *ibid* **44**, 322 (1984).
- 7) C. H. Yang, J. M. Carlson-Swindle, S. A. Lyon, and J. M. Worlock, *Phys. Rev. Lett.* **55**, 2359 (1985).
- 8) M. Helm, E. Colas, P. England, F. DeRosa, and S. J. Allen, Jr., *Appl. Phys. Lett.* **53**, 1714 (1988).
- 9) A 100 Å-thick NiCr heater was evaporated on one surface of a 125 μm-thick sapphire substrate (2×3 mm²) and a AuGe thermometer layer was deposited on the other face. The FIR radiation was generated by applying 1 Hz square wave voltages, while the temperature was synchronously monitored by measuring the resistance of the AuGe film.
- 10) The length of the voltage pulses was limited by the bolometer response frequency (~1 kHz).
- 11) K. Hirakawa and H. Sakaki, *J. Appl. Phys.* **63**, 803 (1988).
- 12) P. W. Kruse, L. D. McGlauchlin, and R. B. McQuistan, *Infrared Technology* (John Wiley and Sons, New York, 1962).
- 13) R. A. Hopfel, E. Vass, and E. Gornik, *Solid State Commun.* **49**, 501 (1984); R. A. Hopfel and G. Weimann, *Appl. Phys. Lett.* **46**, 291 (1985).
- 14) N. Okisu, Y. Sambe, and T. Kobayashi, unpublished.
- 15) The upper temperature limit in the present experiment is not an intrinsic limit of the FIR technique, but rather due to lattice heating and/or ohmic contact problem.
- 16) F. Stern, *Phys. Rev. B* **5**, 4891 (1972).
- 17) K. Hirakawa and H. Sakaki, *Appl. Phys. Lett.* **49**, 889 (1986).